A BALLOON-BORNE INSTRUMENTATION FOR COSMIC GAMMA-RAY BURST DETECTION AND MEASUREMENT

G. VENTURA, H.M. HORSTMAN, A. BRIGHENTI,
C. CAVANI, M. CAMPRINI, P. CAZZOLA,
G. GIOVANNINI, C. LABANTI, and J.M. POULSEN

Istituto di Tecnologie e Studio delle
Radiazioni Extraterrestri
Via Castagnoli, 1. 40126 Bologna, Italy

Submitted for publication to
Nuclear Instruments & Methods

JANUARY 1984

RAPPORTO TECNICO N° 98
NOTA TECNICA

ABSTRACT

A wide-field X-ray detector for observations of cosmic gamma-ray bursts has been prepared and launched on a balloon platform from the base of Trapani-Milo (Sicily) in July of 1983. The detector is an imaging type, a 40 cm diameter gamma camera, paired with a 1.8 m diameter pseudorandom, 50% open mask, to make up the telescope. The detector works in the energy range between 30 and 600 keV with imaging capabilities up to 300 keV. A description is given of the detector characteristics, main payload electronics and also the supporting packages and subsystems.

1. Introduction

The astronomy of γ-ray bursts has been developing rapidly in the past few years. Detectors on a large scale network of satellites and interplanetary probes [1] have led, for the more intense bursts (more than 10^{-5} erg/cm^2), to more and more precise localizations of the sources. Even with the precision obtained, however, few possible identifications have emerged [1,2,3].

The use of a number of larger area detectors placed on the Venera 11 and 12 probes [4], repeated later on Venera 13 and 14, reveal the presence of a large number of less intense bursts ($\gtrsim 10^{-7}$ erg/ cm^2). These observations indicate that the sources are more or less isotropically distributed in the sky (one probe gives 1-3 deg source localization) and moreover reveal the presence of repeating sources and of interesting features [5,6,7]. The spectral analysis shows a possible broad cyclotron absorption or emission line and a feature near 420 keV in emission which can be interpreted as a gravitationally shifted positron electron annihilation line. There has been some discussion on the reality of the cyclotron line [8,9]. In any case the spectral form has been observed as being rapidly variable and episodic in nature with the annihilation line or the cyclotron feature appearing, disappearing and reappearing during the event on a time scale of $\lesssim$ 0.1s [10]. There is also the 23 msec quasi-periodic variation observed in the spike of the March 5,1979 burst [11]. In the same burst the long term history can

also be extremely interesting: the initial, intense, 0.1 sec spike was followed by an 8 sec oscillation for minutes afterwards [12]. As will be seen below, we have tried to cover as well as possible with the data handling on-board the various time intervals involved from 0.5 ms to minutes.

The use of a gamma camera and a coded mask for burst observation and localization was first proposed at the Innsbruck Cospar meeting [13] in connection with a then possible spinning Italian satellite. We have since developed a design for balloon use which attempts to permit observation of the spectral features mentioned above on relatively fast time scales allowing simultaneously observations of bursts to lower fluences and spatial localizations to 5 to 10 minutes of arc.

In what follows, we will describe briefly the operations of the gamma camera and, in more detail, the payload electronics, the burst memory, the telemetry and trigger CPU and the aspect sensors.

2. Payload configuration

The system flight configuration is shown in fig. 1.The gondola structure is a prism with a dodecagon cross section mounted on top of a cube which holds the telemetry and the ballast packages. The gondola has a diameter of 1.9 m and a height of 1.5 m; its weight is 800 kg when ballast is included.

The detector is essentially cylindrical and its axis is aligned with the geometrical axis of the structure together with the high voltage unit which is placed under the detector. The mask

is 40 cm above the detector.

The azimuth control system used a horizontal magnetometer to position the gondola with respect to the magnetic field. Six stainless steel cables connected the corners of the structure to the attachment points of the azimuth drive motor.

The sun follower (SF) was placed on the south side of the gondola protruding 0.5 m from the structure. The star sensor or CCD camera (SS) was fixed inside the gondola at 29 deg from the horizontal and about 90 deg East. Alignment tests were performed on the ground to calibrate more precisely the positio= ning of the aspect sensors.

Electronic packages and battery boxes were positioned inside the gondola to distribute the weights and balance the payload.

3. Flight instrumentation

Fig. 2 shows the functional block diagram of the payload. In the gondola system, the following blocks can be identified:

(i) the telescope and associated electronics;

(ii) azimuth control system (ACS);

(iii) aspect sensors (SF and SS);

(iv) service electronics (SE);

(v) data handling system (DHS) with burst trigger and memory CPUs.

These will be described in some detail below.

3.1 The telescope and associated electronics

Coded masks, consisting in part of X-ray absorbing elements

and in part of openings, have been used some times in the past in combination with position sensitive detectors to allow the reconstruction of sky images. The problems pertinent to balloon flights have recently been discussed by Cardini et al. [14].

In our instrument the design of the mask was conditioned and simplified by other considerations (see table 1 for details). A large field of view was desired, and a quarter of the sky is given by a half-opening angle of 60 degrees. Up to this angle a full shadow of the mask was desired on the gamma camera. It is, however, to be considered that hard X-rays can have several millimeters of average stopping length in the NaI crystal, and therefore are detected with a position error when coming in at large angles. The thickness of the lead elements in the mask was then chosen as 5mm, a choice which allows good shadows up to 200 keV and a partial transmission at 300 keV, the upper limit for X,Y position data. At 60 degrees the shadow for a 5mm thickness is 1 cm in the case of completely absorbed events. This suggested a size of the basic element of 1.5 cm, a bit longer than the shadow mentioned above. In this way it is possible to distinguish two lead elements separated by one unit hole, even for 60 degree incident radiation.

Setting the diameter of the mask to 1.80 m, the size of an automatic programmable drilling machine, the distance of 40 cm from the mask to the detector is fixed.

More complete details on the mask and the detector plane will be given elsewhere (papers to be submitted for publication).

Main detector characteristics are shown in table 2. As depi=

cted in fig 3, the detector is seen by 19 photomultipliers through a lightpipe. The photomultipliers are supplied with individual high voltage dc-dc converters which are enclosed in a separate pressurized container to protect the crystal from overheating. This facilitates single tube gain adjustments as the detector container remains always closed and light tight. The PMT anodes were connected to ground and the analog circuits were all direct coupled allowing high counting rates to be followed with precision.

The 19 outputs V_i from the preamplifiers are fed to the EXY electronics box, which gives three data for the energy, the X- and Y-position of each detected photon within a fixed energy window (30-300 keV). The functional block diagram of the EXY electronics is shown in Fig. 4.

The photon energy E is given by the sum of the 19 signals, and the Y-position is calculated as the geometric mean:

$$\langle Y_1 \rangle = \sum_i y_i \cdot V_i \qquad (1)$$

$$\langle Y \rangle = \langle Y_1 \rangle / E \qquad (2)$$

where the weights y_i are the same for all the phototubes in the same row (see fig. 3). The division in (2) is performed in two different ways giving analog and digital outputs. The analog division is performed with an analog divider. <Y> signal, together with the corresponding <X> signal and a "pulse presence" signal, can be sent to an oscilloscope to form a quick-look image of the gamma camera . The X-position was derived from the following

relation:

$$\langle X \rangle = \langle A + B \rangle / 2 E \cos 30 \qquad (3)$$

where A and B are calculated with the same algorithm as $\langle Y_1 \rangle$ along the symmetry axes α and β shown in Fig. 3.

It would have been possible to send all the 19 signals to separate ADC's and transmit the converted signals. This leads, however, to a weighting and a division of the signals after the flight whose accuracy would depend on the pulse height and hence on the energy of detected X-ray. It leads as well to an excessive number of bits to be transmitted and to a large dead time. On the other hand, it is rather difficult to implement analogue divisions with accuracy and independently of the pulse-height. The digitized information of the signal (2) and (3), i.e. the division of the unnormalized position signals $\langle Y_1 \rangle$ and $\langle A+B \rangle$ with the energy signal E, is accomplished in ADCs whose "voltage reference" inputs are fed by the stretched signal E_1. In this way the accuracy of the on-board division depends only on the statistical fluctuations of the signals and on the success in eliminating DC offsets at the input of the ADCs. 8-bit successive approximation ADCs were used with the sliding scale correction method [15]. Ground tests of the divider showed a differential non-linearity of about $\pm$ 0.4%. For each event, digitized data E^*, X^*, Y^* and the time t^* (with a 20 μsec resolution), are telemetered in the form of four-8-bit words. The bin size is about 1.5×1.5 mm.

The EXY electronics is frequency limited to about 80 kcps, while information on the integral counting rates up to 0.5 Mcps is available.

3.2 Azimuth control system (ACS)

The ACS works with the signal from a horizontal magnetometer to position the gondola with respect to the local magnetic field within ± 0.5 deg. The magnetometer was aligned before launch with the N-S direction. The gondola is below the driving motor which is attached to the parachute shrouds.

3.3 Sun follower (SF) and star sensor (SS)

For the localization of a burst, the knowledge of the position of the detector with a higher precision than that furnished by the ACS is needed. For this purpose a sun follower (SF) and a CCD camera (SS) were constructed and included in the payload, for day and night operation respectively.

The sensor of the sun follower was a four quadrant diode placed in a tube to shield it from stray reflections. It was mounted on an equatorial mount with the latitude set arbitrarially at 40 deg and placed on the southern side of the structure. Two motors, which could be used either in manual or automatic mode, gave the drive in hour angle and in declination.
Initially the manual mode was used to point the sun with the help of the housekeeping telemetered data which gave sun illumination. Once this signal was peaked up, one changed from the manual mode to the authomatic mode. Each shaft of the SF was mechanically coupled through a doubling device to a 12 bit shaft encoder. During the flight the position of the sun relative to the gondola was then given with a precision of 3 arcmin in both hour angle and declination.

For night operation a CCD based star sensor was employed. The position of the SS in the gondola was chosen so as not to have the moon in the field of view at the launch date. We essentially had a camera with a NIKON 50 mm f/1.2 lens and a field of view of about 7×9 deg^2 at the position of the CCD. The sensor was cooled by a Peltier device to about 30 deg below the ambient temperature; the CCD pixels were 1.5×1.5 arcmin^2 and, with the movement of the gondola, a star in the sensor field would produce a short horizontal track. The device gave the position of the maximum intensity pixel for two stars in its field of view together with star magnitudes. Once a star is detected, the device is able to track it automatically. Position and magnitude data are renewed every 70 msec and transmitted. The sensor was expected to reveal stars down to the 5-th magnitude. The night data have not yet been fully analyzed.

3.4 Service electronics (SE)

As is shown in fig. 2, the tasks to be performed by the SE are the following:

1) low voltage power distribution;
2) subsystem analog and digital housekeeping data collection, pre-processing and organization;
3) discrete telecommand latching and activation; parallel T.C. word handling for the DHS;
4) pulse height analysis of the sum pulse E incoming from the EXY box for energies between 280 and 600 keV (Extended Energy Range).

3.5 Data handling system (DHS)

The design of the DHS was strongly conditioned by the maximum allowable bit rate at Trapani (34 kbit /s), which is already insufficient for transmission of the expected background data in real time. The DHS was implemented around two CPUs: the Burst Trigger CPU and the Burst Memory-Telemetry CPU (Master Processor).

The Burst Trigger CPU has to recognize if a burst has occurred, i.e. if the current counting rates are higher than the actual trigger settings. Furthermore, to detect different time evolutions of bursts and, in particular, different burst rise times, the comparision of counting rates are performed on the three time scales 4, 32 and 256 msec. The Burst Trigger CPU logical operation is shown schematically in fig. 5 and its implementation in fig. 6. Incoming pulses from the EXY box, Emin<E<Emax, are averaged on the three selected time scales to give the actual M4, M32, and M256 counting rates. The corresponding σ values are calculated using a look-up table written in an EPROM which uses the counts N4, N32, N256 accumulated in 256 msec, 32 sec before the present time. The algorithm is shown in fig. 5. When the present count exceeds the old value by a given number of σ, the trigger fires and a flag code is sent to the Master Processor. The number of σ for each time base can be set by parallel telecommands. Two types of T.C. could be sent: orders, such as system reset/set and mode controls, and data, such as a new sigma

value. In each case when a T.C. is sent, the interrupt line of the burst CPU is activated and the telecommand data is processed. To avoid ambiguity and increase noise immunity, an 8-bit T.C. was broken into two-4-bit words which were handled as shown in fig. 5. A single 8-bit command was used to send orders to the DHS while two successive bytes were needed to change a sigma value. In the last case, the first command says which level is to be changed, while the second sets the new value in the selected range. T.C. actual status is always echoed through the telemetry link. The Burst Trigger & T.C. processor was built around a Z80 CPU and features a 2 kbyte RAM, a 2 kbyte EPROM, a PIO for the T.C. input, a PIO for the output data to the master CPU and a CTC for the timing control. The priority interrupt assignment for the 4 msec timer and the input port is indicated in fig. 6.

The Master Processor can work in three modes; for each of them a particular telemetry format is generated:

a) Normal mode (NM) in which the counting rates do not exceed the burst thresholds; about 75% of the format is reserved to X-ray absorption data, i.e. X^*, Y^*, E^* and event time t^*, with a dead time of about 50% for an expected background of 1500 cps. Transmitted event data will be indicated from

here on as a vector data $\theta = (X^*, Y^*, E^*, t^*)$.
Integral counting rates with a 4.23 msec time resolution, EER spectra, aspect sensors and housekeeping data are also telemetered. Burst counters and sigma levels are transmitted as housekeeping data as well as frame counter and on-board time with a 20 μsec resolution.

b) Burst mode (BM) in which at least one of the trigger levels has been exceeded and burst code has been activated by the burst trigger CPU. θ data are not telemetered but stored in the burst memory. 50% of the format is reserved to integral counts at high time resolution ($\sim$ 0.5 msec) and to EER data at a time resolution of 0.53 sec for a 256 channel spectrum. Other housekeeping data are transmitted as in NM. The time needed to completely fill the 1.5 Mbyte burst memory obviously depends on the burst counting rate. This memory size permits storage of $3.2 \cdot 10^5$ events/burst. About $64 \cdot 10^3$ events relative to the pre-burst history are stored in a 256 kbyte memory to overcome NM dead time limitations. Once the burst memory is filled, the DHS is ready to transmit the stored burst and pre-burst data. Even after the burst memory has been filled, the DHS goes on for several minutes in BM to observe possible burst tails [12].

c) Memory transmission (MT) is identical to NM except for the fact that the θ vectors are not the actual data relative to X-ray absorption in the crystal, but those stored in the burst memory during burst occurrence. At the 34 kbit/s bit rate the time needed to transmit the whole memory content

is about 10 min. During this time, incoming data from the detector are lost except for the integral counts. Some characteristic of main telemetered data are summarized in table 3.

To facilitate quick look and data analysis, the main frame was organized as 32 8-bit words for the three modes while sub-commutated formats could be changed as needed. As depicted in fig. 6, the master processor is a Z80 family based system bundled with 2kx8 RAM, 2kx8 EPROM, several PIO, CTC, DMA controller with logic and a 1.5 Mbyte burst data memory.

Since data loss in the transmission bit-stream generation was thought to be undesirable, the highest interrupt priority was reserved to the programmable timer CTC 4 which produces the telemetry waveforms, i.e. bit and word rate. Lower priority levels (IP 2 through IP 10 shown in fig. 6) were assigned to the other I/O ports. When operating in BM, the master processor has to handle a large amount of high frequency, random data and store them into the 1.5 Mbyte memory, which is organized in 32 kbyte segments. The data direct flow supervision into memory was assigned to the DMA controller and to the DMA logic, while other data are continuously formatted and transmitted by the master CPU. While θ data are beeing stored into the burst memory, the burst time evo= lution is followed by inserting timing information into the memory. For this reason, every 5 msec a vector T=(Tμs,Tms,Ts,Tm) substitutes a θ vector. Instead of removing periodically the

system from the DMA control, which would have produced a loss of data, it was decided to purely "decoy" the DMA chip with the help of the DMA arbitration logic depicted schematically in fig. 7. The DMA is programmed to transfer data blocks of 32 kbytes; during a single autorepeat block storage, every 5 msec the time vector T, furnished by CTC 3, is stored in memory as if it were a θ vector data coming from the relative PIO, simply swapping the hardware address selection of these ports. When a 32 kbyte block is completed, the DMA sends an interrupt to the CPU which updates the new segment memory address and gives again the bus control to DMA.

4. Ground support equipment (GSE)

A Cromemco computer was used for laboratory testing and calibration of the instument as well as for data real time quick-look during the flight. Based on a Dual Processing Unit and with a 256 kByte memory capacity, the computer is equipped with standard peripheral devices: dual floppy disk, printer, video display and I/O homemade interfaces.

In both the main tracking ground stations, Milo and Palma de Mallorca, a Cromemco computer was used in conjunction with a Conic D-PAD III bit synchronizer, which gave scientific format data as parallel 9-bit words; the "quick-look" computers were also connected to the ground Telecommand Encoder Units.

Processed incoming telemetry data were then display-

ed and printed to give a quasi-real time control of onboard system operations while, at the same time, it was possible to send parallel, software-programmed telecommands through the operator keyboard.

Scientific data from the bit synchronizer were also continuously recorded in digital form at Milo, using a HP-21MX computer, while only analog recording of the data bit-stream was possible at Palma and downstream at Arenosillo.

In all cases IRIG-B time standard code generators were employed to get precise time data phasing.

5. Pre-flight calibration

After the principal components of the package were mounted at Milo, the gondola was carried out into the open field and its north-south axis was aligned to the geographic north-south line. At this point the telemetry and the SF were turned on and data was taken near local solar noon from the two shaft encoders of the sun sensor. From this data it will be possible to calculate rather precisely the relative positions of the SF and the gondola structure. The zeroes of the shaft encoders will also be found in this set of data (mechanically they were set to zero at zero hour angle and declination).

The gondola was then rotated about 120 deg clock-wise to bring Jupiter into the field of view of the

SS at about 23.00 local time on the 16th of july, 1983. The SF was then turned on in the automatic mode again. The recorded data from the SF in this period can be used to determine the new position of the gondola. The position of the SS relative to the gondola is then determined from the night run on Jupiter.

More precise relative positions of the SF, SS and the mask can be determined using these ground calirations and the sky positions observed during the flight for the stronger sources such as the Crab and Cyg X-1.

6. Conclusions

The experiment was launched from the balloon base of Trapani-Milo (Sicily) on the 26th of July and recovered in Spain after a 20 hour flight.

Owing to the failure of the detector window during the ascent of the balloon, most of the observation time was lost. This was due to the fact that the external thermal protection of the payload was not light tight and the sun light illuminated the detector, completely masking X-ray signals. In the last part of the flight, after sunset, the system was again able to detect X-ray events and to transmit main information to the ground stations.

All the subsystems (electronics, aspect sensors, azimuth control system etc.) worked as expected during the whole flight.

Data relative to the final part of the transmediterranean flight are at present being processed so experimental results are not yet available.

Since from a preliminary look at night data, which gave a background count rate of about 1.24 count s^{-1} cm^{-2} at an altitude corresponding to 9 mbar, it is to be presumed that the count rate at the desired float altitude was less than the expected. This rather low altitude was in part due to a leaky balloon and in part to the beginning of the night.

After the repair of the detector and a few changes in the subsystems, we plan to fly the detector again in the summer of 1984 with the same scientific objectives of the 1983 flight.

In the future the same experiment could also be rearranged to perform measurements of hard X-ray sources in the energy range 30-300 keV.

Acknowledgements

We would like to express our gratitude to many people who helped us with valuable ideas and made possible the realiza= tion of the experiment. Among them, we would like to parti= cularly thank Dr. G.Cavallo for the help in the early manage= ment of the experiment; Dr.G.Pizzichini for the prelimina= ry contribution and suggestions on "burst phenomenology"; Dr. W.Dusi and G.Landini for the set-up of the azimuth control system; A.Rubini, O.Catani, S.Silvestri and Dr.M. Trifoglio for the assistance at the base of Milo; E.Rossi and S.Traci for the construction of some parts of the payload. Particularly warm thanks are to be expressed to Dr. C.R.Butler for his competent contribution during the flight. Thanks are also due to E.Banfi (Laben Co.) for the realization of the EXY electronics; to the firm Carpigiani for the cooperation in the construction of the mask; to ESTEC and to the firm GALILEO for the collaboration which permitted the use of the star sensor; to ESA for the fellowship given to J.M. Poulsen in 1982. Finally we are grateful to the Milo base and to the CNES staff for the excellent cooperation before and during the flight. The financial support to this experiment was mainly furnished by the Italian Space Plan (PSN) of the National Research Council (CNR).

References

[1] T.L. Cline, Adv. Space Res. 3(1983)175

[2] H. Pedersen et al., Ap.J. (Letters) 270(1983)L43

[3] B.E. Schaefer et al., Ap.J. (Letters) 270(1983)L49

[4] E.P. Mazets et al., Astroph. Space Sci. 80(1981)1

[5] E.P. Mazets et al., Astroph. Space Sci. 84(1982)173

[6] E.P. Mazets et al., Astroph. Space Sci. 82(1982)261

[7] B.J. Teegarden and T.L. Cline, Ap.J. (Letters) 236 (1980)L67

[8] E.E. Fenimore, R.W. Klebesadel and J.G. Laros, Proc. XXIV COSPAR, Preprint LA-UR-82-1883(1982)

[9] J.P. Lasota and B.M. Belli, Nature 304(1983)139

[10] U.D. Desai et al, Proc. 18th I.C.R.C.,Bangalore, XG-2(1983)43

[11] C. Barat et al., Astron. and Astroph. 126(1983)400

[12] E.P. Mazets et al., Nature 282(1979)587

[13] H.M. Horstman et al., (COSPAR) X-Ray Astronomy, Ed. W.A. Baity and L.E.Peterson (1979) 539

[14] D. Cardini et al., Astron. and Astroph. 127(1983)169

[15] C. Cottini, E. Gatti and V. Svelto, Nucl. Instr. and Meth.24(1963)241

Table 1

Telescope characteristics and features.	
1/2 cone opening angle	60 degrees
Mask	Random with 10340 elem. 50% open, 1.8 m diam.
Unit mask element	Pb $1.5 \times 1.5 \times 0.5$ cm^3
Detector plane (NaI Crystal)	43 cm diam, 12 mm thick
Mask detector distance	40 cm
Basic angular resolution	2×2 deg^2
Number of pixels in a sky image	6669
Energy range (with imaging)	30 - 300 keV
" " (without imaging)	300 - 600 keV
Energy resolution (%,FWHM)	20.0, @ 60 keV, Am241
" " " "	12.0, @ 279 keV, Hg203
" " " "	15.5, @ 511 keV, Na22

Table 2

Detector characteristics	
NaI(Tl)	43 cm diam., 1.2 cm thick. ~ 1200 cm^2 area
F2 lead glass (light pipe)	54 cm diam., 3.0 cm thick.
PMTs	9761 EMI, 9.2 cm (3.5") diam.
Al- window	45 cm diam., 0.5 mm thick.
Position resolution of detector	~ 10 mm (fwhm) at 60 keV
Detector weight including housing	120 kg
High voltage supply unit weight	35 kg

Table 3

Telemetered data(0)	Time resolution(1) (msec)		Max Allowable(2) Intensity (cps)		Dead time(3) (%)	
	NM	BM	NM	BM	NM	BM
Single events	1.32	-	700	-	50	-
Integral counts(4)	4.23	0.53	60000	480000	~0	~0
EER spectra(5)	2.17 s	0.53 s	30000	120000	~0	~0
SF encoders(6)	33	33	-	-	-	-
SS(7)	70	70	-	-	-	-

(0) @ 34 kbit/s bit rate; word size is 8 bit + 1 parity bit
(1) data relative to NM & BM Formats. See also in the text
(2) max intensity at the 8-bit word capacity
(3) corresponding to a 1500 cps background
(4) flat spectra is assumed to be equally distributed in the 30-300 keV range
(5) 256 channel spectrum; 280 keV<E<600 keV
(6) two-12 bit data words
(7) two stars coordinates and magnitudes

Figure Captions

Figure 1. Payload pre-flight configuration.

Figure 2. Functional block diagram of the payload with main electrical connections in evidence.

Figure 3. Photomultipliers as seen looking from bottom of the detector with Y, X, α and β symmetry axes. The numbers on the left are the weights y_i assigned to the PMs.

Figure 4. Block diagram of the detector electronics. Signals V_i come from the detector; data on the right hand are fed to the Master CPU.

Figure 5. Flowchart of the Burst Trigger CPU. The logical operation is based on the interrupt request coming automatically from a timer or upon a telecommand reception.

Figure 6. Data Handling System electrical block diagram. The system is built around two Z80 CPU: one handles the burst trigger, the other controls the data addressing, the memory management and the analog housekeeping data together with the telemetry format generation.

Figure 7. Direct Memory Access arbitration logic electrical schematic with waveforms involved.

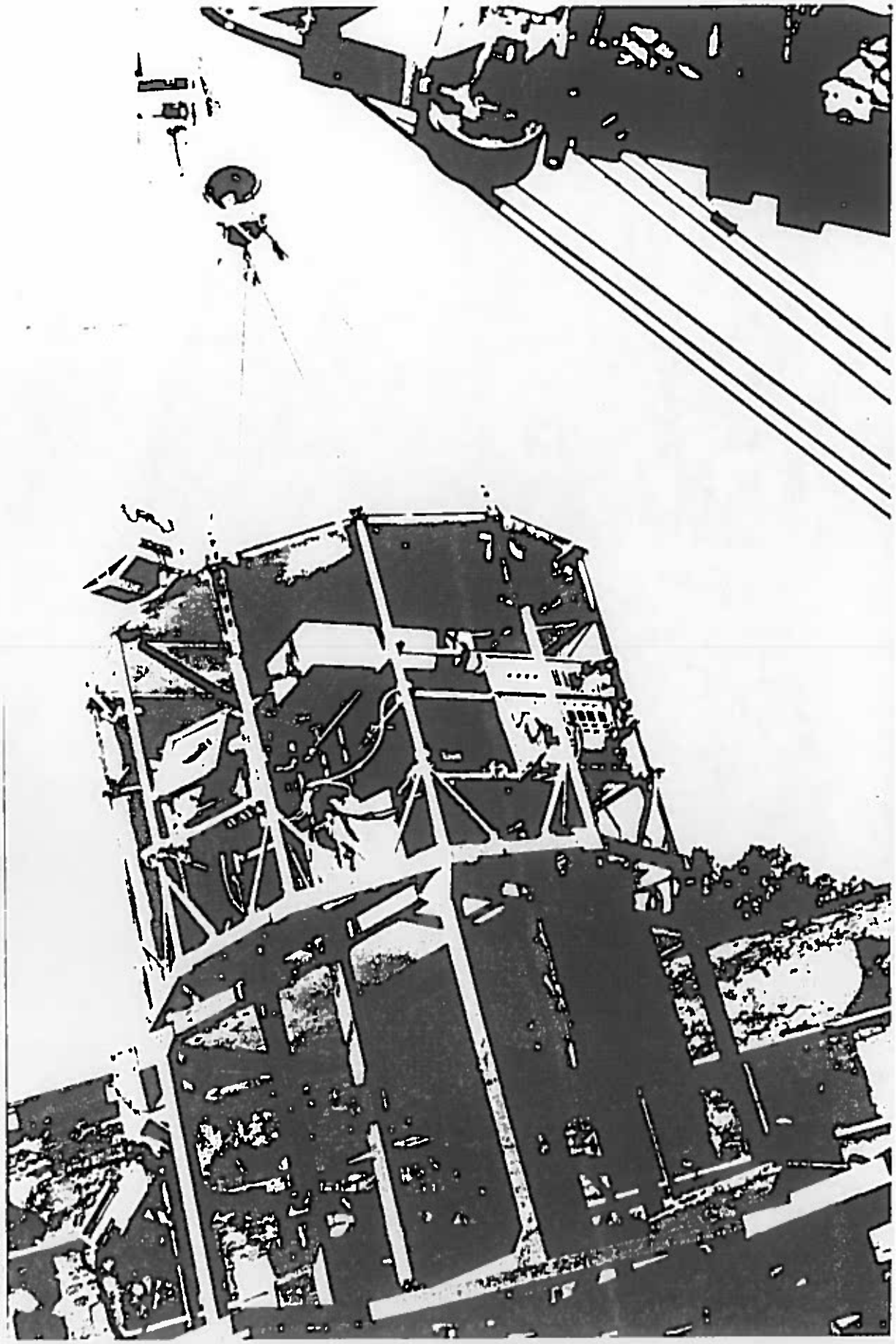

Fig. 1

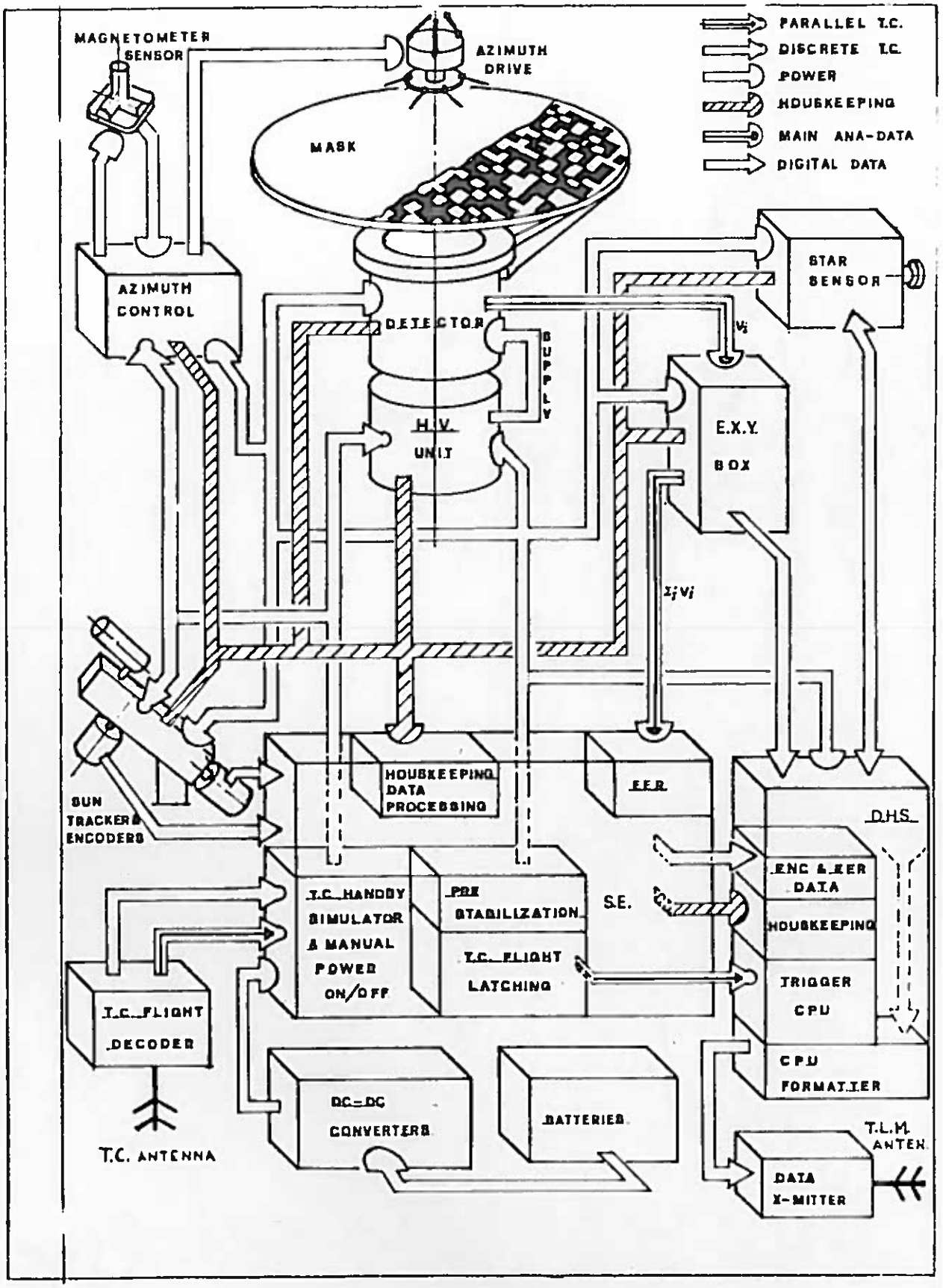
PARALLEL T.C.
DISCRETE T.C.
POWER
HOUSKEEPING
MAIN ANA-DATA
DIGITAL DATA
MAGNETOMETER SENSOR
AZIMUTH DRIVE
MASK
AZIMUTH CONTROL
STAR SENSOR
DETECTOR
SUPPLY
H.V. UNIT
E.X.Y. BOX
HOUSKEEPING DATA PROCESSING
EER
DHS
SUN TRACKER & ENCODERS
T.C. HANDBY SIMULATOR & MANUAL POWER ON/OFF
PRE STABILIZATION
T.C. FLIGHT LATCHING
S.E.
ENC & EER DATA
HOUSKEEPING
TRIGGER CPU
CPU FORMATTER
T.C. FLIGHT DECODER
T.C. ANTENNA
DC-DC CONVERTERS
BATTERIES
T.L.M. ANTEN
DATA X-MITTER

Fig. 2

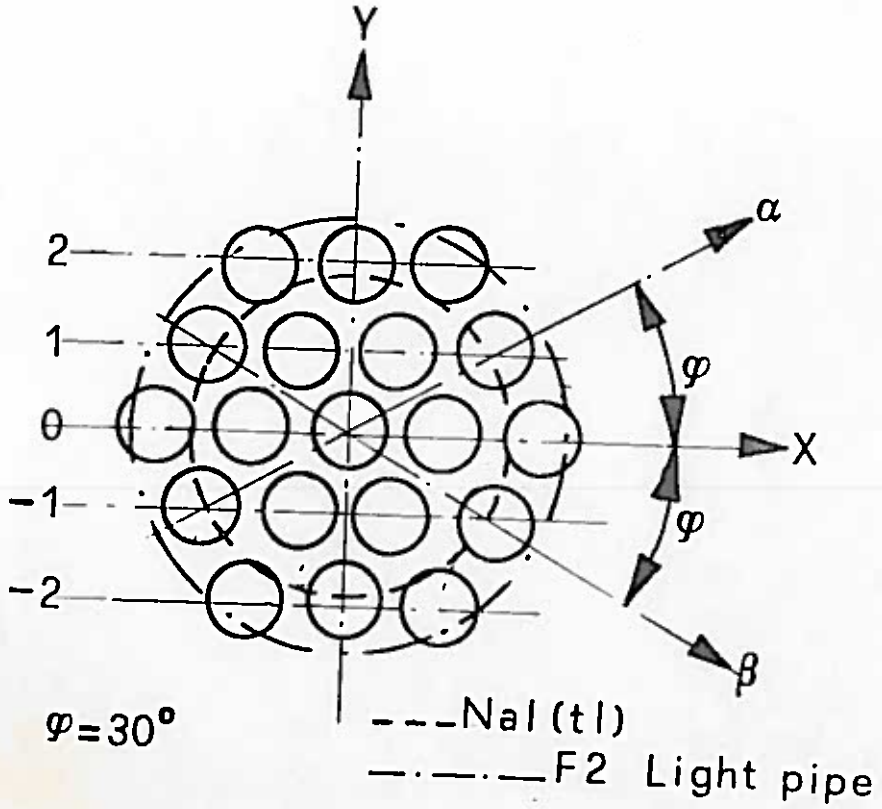

Fig. 3

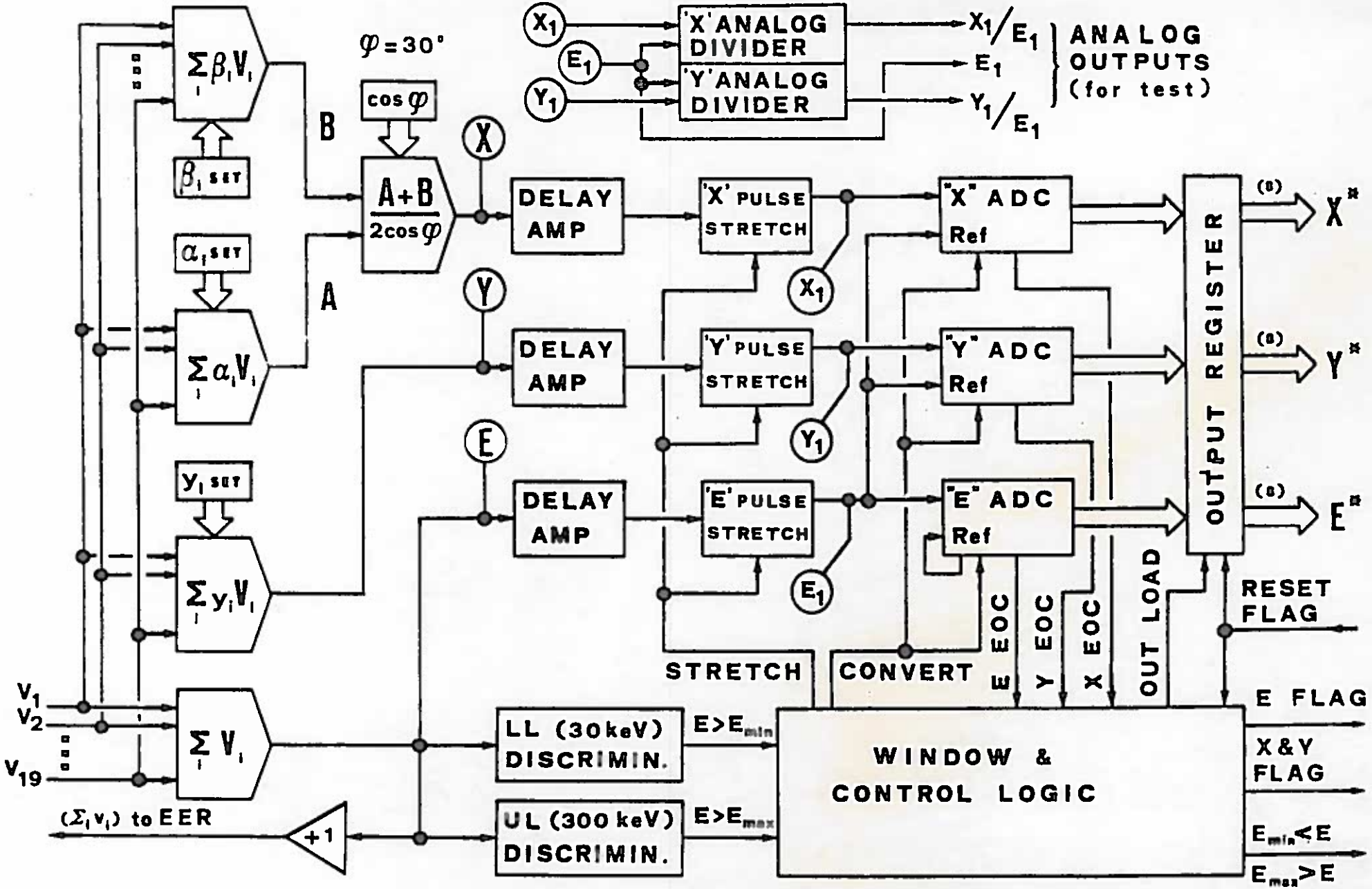
$\varphi = 30°$
$\cos\varphi$
$\frac{A+B}{2\cos\varphi}$
$\Sigma_i \beta_i V_i$
β_i SET
$\Sigma_i \alpha_i V_i$
α_i SET
$\Sigma_i y_i V_i$
y_i SET
$\Sigma_i V_i$
V_1
V_2
V_{19}
$(\Sigma_i v_i)$ to EER
+1
A
B
X
Y
E
X_1
E_1
Y_1
'X' ANALOG DIVIDER
'Y' ANALOG DIVIDER
X_1/E_1
E_1
Y_1/E_1
ANALOG OUTPUTS (for test)
DELAY AMP
DELAY AMP
DELAY AMP
'X' PULSE STRETCH
'Y' PULSE STRETCH
'E' PULSE STRETCH
"X" ADC Ref
"Y" ADC Ref
"E" ADC Ref
OUTPUT REGISTER
(8)
(8)
(8)
X^*
Y^*
E^*
STRETCH
CONVERT
E EOC
Y EOC
X EOC
OUT LOAD
RESET FLAG
LL (30keV) DISCRIMIN.
UL (300 keV) DISCRIMIN.
$E>E_{min}$
$E>E_{max}$
WINDOW & CONTROL LOGIC
E FLAG
X&Y FLAG
$E_{min}<E$
$E_{max}>E$

Fig. 4

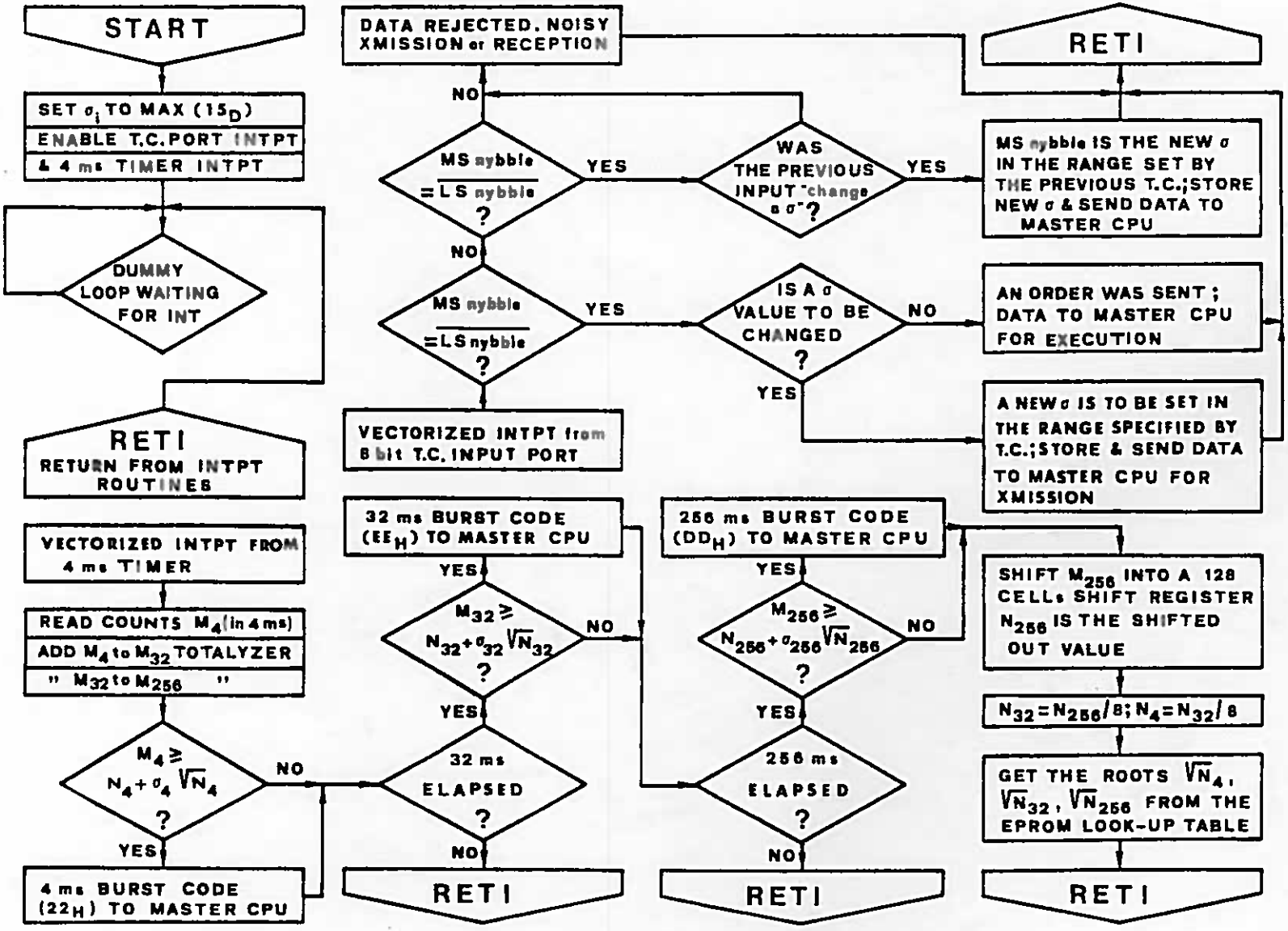
START
SET σ_i TO MAX (15_D)
ENABLE T.C.PORT INTPT
& 4 ms TIMER INTPT
DUMMY LOOP WAITING FOR INT
RETI
RETURN FROM INTPT ROUTINES
VECTORIZED INTPT FROM 4 ms TIMER
READ COUNTS M_4 (in 4 ms)
ADD M_4 to M_{32} TOTALYZER
" M_{32} to M_{256} "
$M_4 \geq N_4 + \sigma_4 \sqrt{N_4}$?
YES
NO
4 ms BURST CODE (22_H) TO MASTER CPU
DATA REJECTED. NOISY XMISSION or RECEPTION
NO
MS nybble = LS nybble ?
YES
NO
MS nybble = LS nybble ?
YES
VECTORIZED INTPT from 8 bit T.C. INPUT PORT
32 ms BURST CODE (EE_H) TO MASTER CPU
YES
$M_{32} \geq N_{32} + \sigma_{32} \sqrt{N_{32}}$?
NO
YES
32 ms ELAPSED ?
NO
RETI
256 ms BURST CODE (DD_H) TO MASTER CPU
YES
$M_{256} \geq N_{256} + \sigma_{256} \sqrt{N_{256}}$?
NO
YES
256 ms ELAPSED ?
NO
RETI
WAS THE PREVIOUS INPUT "change σ"?
YES
RETI
MS nybble IS THE NEW σ IN THE RANGE SET BY THE PREVIOUS T.C.; STORE NEW σ & SEND DATA TO MASTER CPU
IS A σ VALUE TO BE CHANGED ?
NO
AN ORDER WAS SENT; DATA TO MASTER CPU FOR EXECUTION
YES
A NEW σ IS TO BE SET IN THE RANGE SPECIFIED BY T.C.; STORE & SEND DATA TO MASTER CPU FOR XMISSION
SHIFT M_{256} INTO A 128 CELLs SHIFT REGISTER N_{256} IS THE SHIFTED OUT VALUE
$N_{32} = N_{256}/8$; $N_4 = N_{32}/8$
GET THE ROOTS $\sqrt{N_4}$, $\sqrt{N_{32}}$, $\sqrt{N_{256}}$ FROM THE EPROM LOOK-UP TABLE
RETI

Fig. 5

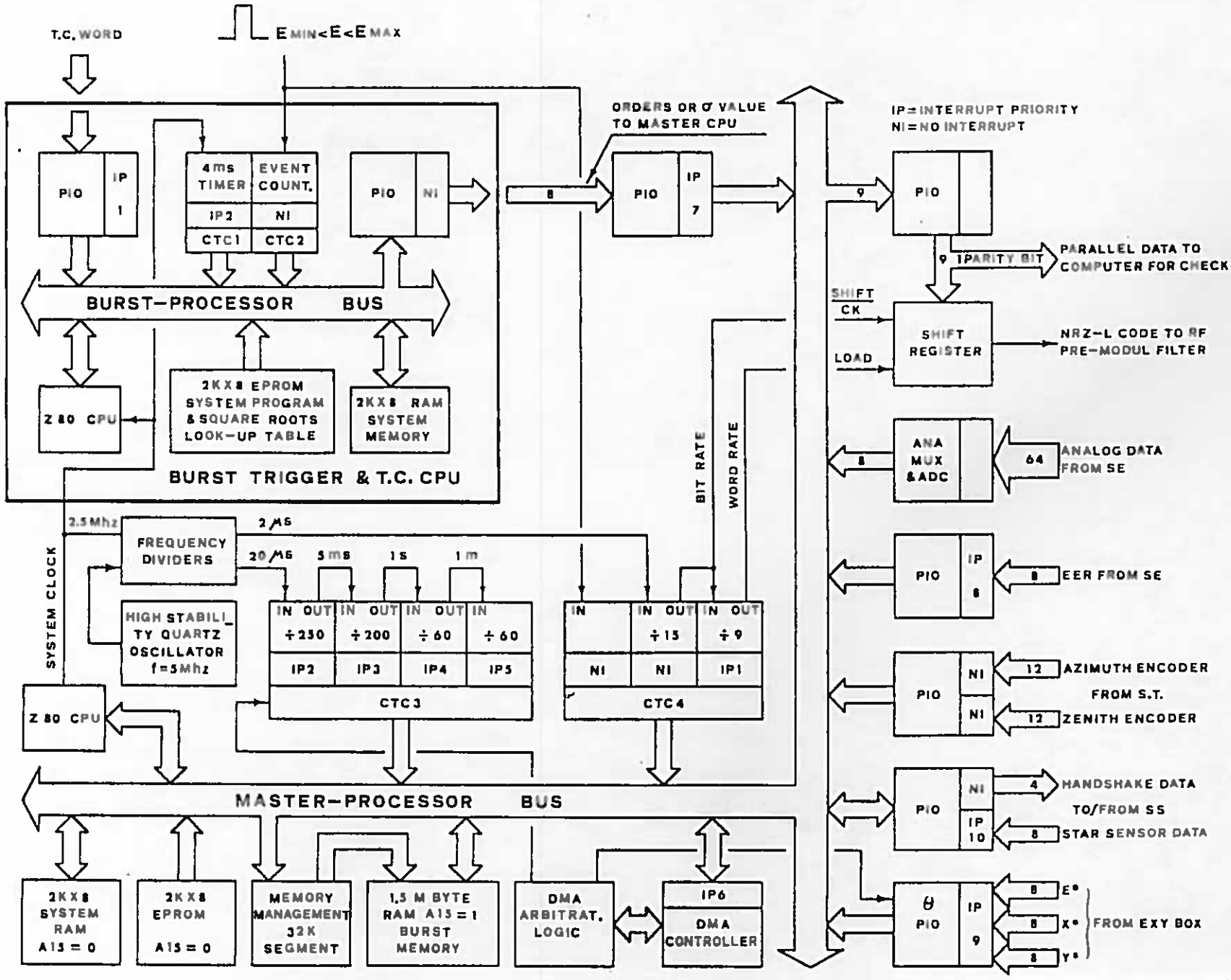
T.C. WORD
EMIN<E<EMAX
ORDERS OR σ VALUE TO MASTER CPU
IP=INTERRUPT PRIORITY
NI=NO INTERRUPT
PIO
IP 1
4ms TIMER
EVENT COUNT.
IP2
NI
CTC1
CTC2
PIO
NI
8
PIO
IP 7
9
PIO
9
PARITY BIT
PARALLEL DATA TO COMPUTER FOR CHECK
BURST–PROCESSOR BUS
SHIFT CK
LOAD
SHIFT REGISTER
NRZ–L CODE TO RF PRE–MODUL FILTER
Z 80 CPU
2KX8 EPROM SYSTEM PROGRAM & SQUARE ROOTS LOOK–UP TABLE
2KX8 RAM SYSTEM MEMORY
BURST TRIGGER & T.C. CPU
BIT RATE
WORD RATE
ANA MUX &ADC
8
64
ANALOG DATA FROM SE
2.5Mhz
SYSTEM CLOCK
FREQUENCY DIVIDERS
2 MS
20 MS
5 ms
1 s
1 m
HIGH STABILITY QUARTZ OSCILLATOR f=5Mhz
IN OUT ÷230
IN OUT ÷200
IN OUT ÷60
IN ÷60
IP2
IP3
IP4
IP5
CTC3
IN
IN OUT ÷15
IN OUT ÷9
NI
NI
IP1
CTC4
PIO
IP 8
8
EER FROM SE
Z 80 CPU
PIO
NI
12
AZIMUTH ENCODER FROM S.T.
NI
12
ZENITH ENCODER
MASTER–PROCESSOR BUS
PIO
NI
4
HANDSHAKE DATA TO/FROM SS
IP 10
8
STAR SENSOR DATA
2KX8 SYSTEM RAM A13 = 0
2KX8 EPROM A13 = 0
MEMORY MANAGEMENT 32K SEGMENT
1,5 M BYTE RAM A13 = 1 BURST MEMORY
DMA ARBITRAT. LOGIC
IP6
DMA CONTROLLER
θ PIO
IP 9
8
E°
8
X°
8
Y°
FROM EXY BOX

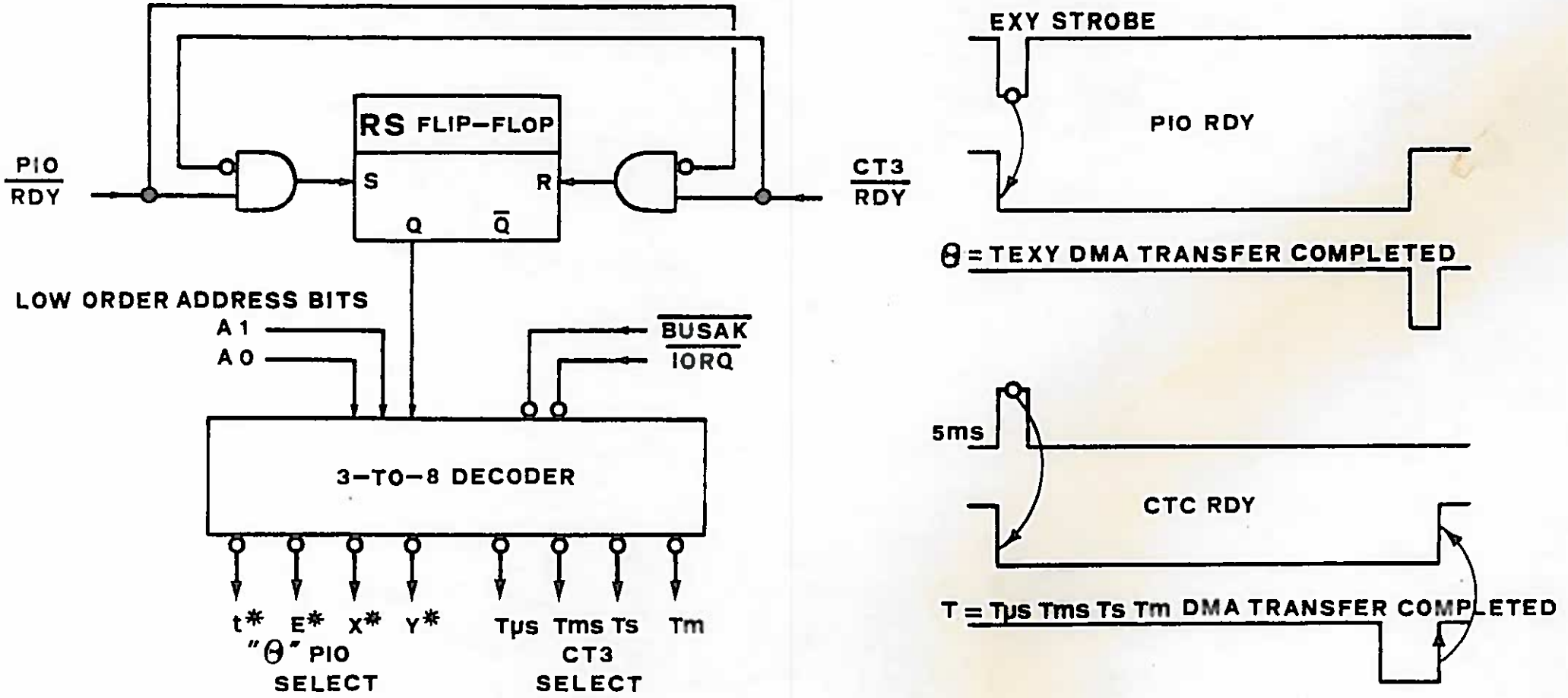
RS FLIP-FLOP
S
R
Q
$\overline{Q}$
PIO RDY
CT3 RDY
LOW ORDER ADDRESS BITS
A1
A0
BUSAK
IORQ
3-TO-8 DECODER
t* E* X* Y*
Tμs Tms Ts Tm
"θ" PIO SELECT
CT3 SELECT
EXY STROBE
PIO RDY
θ = TEXY DMA TRANSFER COMPLETED
5ms
CTC RDY
T = Tμs Tms Ts Tm DMA TRANSFER COMPLETED

Fig. 7